

The present work was submitted to the Faculty of Engineering

# DESIGN OF CHASSIS OF THREE WHEELED ROBOT

## Bachelor Thesis

by

**Munkhgerel Oyunbileg**

Supervisor 1 / Examiner 1

Professor Ph.D. Odbileg Norovrenchin

Supervisor 2 / Examiner 2

Professor Ph.D. Sungchil Lee

Ulaanbatar/Nalaikh, 05/18/2023

## Statutory Declaration

Oyunbileg, Munkhgerel

15348199443696

---

Last Name, First Name

---

Student ID Number

I hereby affirm in lieu of an oath that I provided the submitted bachelor thesis

### DESIGN OF CHASSIS OF THREE WHEELED ROBOT

I did not use any sources other than those stated. In case that the work is additionally submitted on a data medium, I declare that the written and the electronic form are completely identical. The work was not submitted in the same or similar form to any examination authority.

Nalaikh, Mongolia, 05/16/2022

---

Place, Date

*Munkhgerel*

---

Signature

## **Abstract**

This comprehensive study focuses on a three-wheel tadpole configuration consisting of two front wheels and one rear wheel. The research aims to analyze the structural stability of this vehicle design and present a reliable design methodology. To achieve this, a combination of analytical and mathematical approaches was employed throughout the design phase. Advanced software tools, such as Fusion 360, allow for seamless designing and assembly of the vehicle, and the models created were subsequently imported into SolidWorks for further analysis using Finite Element Analysis (FEA) techniques.

As a result, the findings and design guidelines derived from this study can be implemented in the construction of real-life vehicles catering to various transportation needs. Furthermore, the versatility of the three-wheel tadpole configuration opens up possibilities for its utilization in diverse contexts, promoting convenient and efficient transportation solutions.

# Acknowledgement

I want to express my deepest gratitude and appreciation to Mr.Odbileg and Mr.Sungchil Lee for their invaluable guidance and support throughout the course of my graduate thesis. Their insightful feedback, encouragement, and dedication were instrumental in helping me complete this work.

I also extend my thanks to all those who supported me during this challenging journey. Thank you to my family and friends for your unwavering love, encouragement, and motivation. Your support meant everything to me and kept me going through the ups and downs of this thesis.

Finally, I would like to acknowledge the faculty and staff of GMIT for providing me with an exceptional education and the resources necessary to conduct this research. I am grateful for the opportunities and knowledge I gained while at this institution..

## Contents

Abstract .....	3
Acknowledgement .....	4
List of Figures.....	7
List of Table.....	9
1 Introduction .....	10
1.1 Background .....	10
1.2 Limitations .....	11
1.3 Objectives.....	11
2 Methodology.....	12
3 Literature review.....	13
4 Designing and Modelling .....	14
4.1 Mechanic parts.....	14
4.1.1 Chassis.....	14
4.1.2 Suspension.....	16
4.1.3 Steering system.....	21
4.1.4 Encoder .....	23
4.1.5 Wheel design.....	25
4.1.6 Brake .....	26
4.1.7 Motor .....	27
4.1.8 Battery .....	31
4.1.9 Bearing .....	34
4.1.10 Other components .....	35
5 Procedure.....	37
5.1 Modelling.....	37
5.2 Weight distribution.....	38
5.3 Static simulation .....	40
5.3.1 Leaf spring.....	40

5.3.2	Chassis analysis .....	42
5.4	Dynamic simulation .....	46
5.4.1	Terrain ability .....	46
6	Results and Discussion .....	48
6.1	Further study .....	48
7	Conclusion .....	49
8	References.....	50

# List of Figures

Figure 1: Design method flowchart.....	12
Figure 2:Top wireframe of chassis .....	15
Figure 3: Rear wireframe of chassis .....	15
Figure 4: Side wireframe of chassis .....	15
Figure 5: Rear chassis 1.....	16
Figure 6: Rear chassis 2.....	16
Figure 7:Leaf spring with slipper end.....	16
Figure 8: Coil spring .....	17
Figure 9: Right side view of vehicle .....	18
Figure 10: Free body diagram of front chassis .....	18
Figure 11: 3 wheeled tadpole vehicle making left turn.....	21
Figure 12: 4 wheeled automobile making left turn .....	22
Figure 13: Encoder.....	24
Figure 14: Front wheel.....	25
Figure 15: Rear wheel .....	25
Figure 16: Drum brake mechanism .....	26
Figure 17: Front drum brake.....	27
Figure 18: 48V BLDC Motor .....	31
Figure 19: Rear wheel hub bearing .....	34
Figure 20: Front wheel hub bearing.....	34
Figure 21: Chassis bearing.....	35
Figure 22: Differential .....	35
Figure 23: Central U shaped clamp .....	35
Figure 24: Thrust bearing .....	36
Figure 25: Spur gear .....	36
Figure 26: Electric power steering (Model EPS090).....	37
Figure 27: CAD designing structure .....	37
Figure 28: Center of mass of vehicle.....	39
Figure 29: Weight distribution.....	40
Figure 30: Vehicle side view FBD.....	40
Figure 31: Leaf spring safety factor .....	41
Figure 32: Leaf spring stress.....	41
Figure 33: Leaf spring displacement .....	42

Figure 34: Bending test boundary condition .....	42
Figure 35: Chassis displacement bending test .....	43
Figure 36: Chassis stress bending test.....	43
Figure 37: Chassis safety factor bending test.....	44
Figure 38: Torsion test boundary condition .....	44
Figure 39: Chassis displacement torsion test Rear view .....	45
Figure 40: Chassis stress torsion test.....	45
Figure 41: Terrain ability (a) .....	46
Figure 42: Terrain ability (b) .....	46
Figure 43: Terrain ability (c).....	46
Figure 44: Terrain ability (d) .....	47
Figure 45: Terrain ability (e) .....	47
Figure 46: Terrain ability (f) .....	47

## List of Table

Table 1: Material specification .....	14
Table 2: Coil spring specification .....	19
Table 4: Motor specification.....	30
Table 5: Battery specification .....	33
Table 6: List of component mass.....	39

# 1 Introduction

## 1.1 Background

In recent years, robots have been used more and more frequently across a variety of industries. Due to their capacity to maneuver through confined spaces and uneven terrain, three-wheeled robots are commonly used in logistics, material handling, and agricultural sectors. Their chassis design is essential for these robots to operate and perform as intended. This work aims to create a detailed plan for a three-wheeled robot's chassis that meets the stability, mobility, and durability criteria.

Three-wheeled electric vehicles have gained significant attention in recent years due to their possibility to provide sustainable and efficient transportation solutions. Combining the advantages of electric propulsion and a unique three-wheel configuration, these vehicles offer several benefits regarding maneuverability, energy efficiency, and reduced emissions.

### Rising Demand for Electric Vehicles:

- The global electric vehicle market has experienced significant growth in recent years, with an annual growth rate of over 40% from 2019 to 2026. (1)
- In 2020, electric vehicle sales accounted for approximately 4.6% of total global car sales.

### Advantages of Three-Wheeled Configuration:

- Three-wheeled vehicles offer enhanced maneuverability compared to traditional four-wheeled counterparts. They can navigate tight spaces, turn in smaller radii, and offer improved agility in urban environments.
- The reduced number of wheels contributes to lower vehicle weight, resulting in increased energy efficiency and reduced manufacturing costs. (2)

### Energy Efficiency and Reduced Emissions:

- Electric vehicles, including 3WEVs, contribute to a significant reduction in greenhouse gas emissions in contrast with conventional internal combustion engine vehicles.
- According to a study published in the Journal of Power Sources, electric vehicles emit 40-50% less CO<sub>2</sub> over their lifetime compared to gasoline-powered vehicles.

### Market Adoption and Consumer Interest:

- Three-wheeled electric vehicles have garnered attention from both individual consumers and commercial operators.
- Major automotive manufacturers and startups have introduced 3WEV models to the market, indicating a growing interest in this segment.

### Environmental and Urban Mobility Benefits:

- The compact nature of 3WEVs makes them well-suited for urban commuting and last-mile delivery applications, reducing traffic congestion and air pollution. (3)
- A study published in the Transportation Research Part D: Transport and Environment journal highlighted the potential of 3WEVs to improve urban mobility and reduce energy consumption.

The results of this project will help create reliable, practical three-wheeled robots that can significantly increase production and lower costs in various industrial applications and transportation. Firstly, the given vehicle part is inspected, and its dimension is measured by the appropriate method for the first step of the modeling iteration. Next, the estimated model is drawn on Fusion 360 and kinematics, motion analysis, and stress/strain simulation, then the presentation is discussed.

## 1.2 Limitations

One limitation of this complete design and modeling is the vehicle parts given by my institution, which are two front wheels, motor, differential, drum, and shaft. Numerous topic calculations are excluded in this paper, such as differentials, automatization, specific purpose, etc.

## 1.3 Objectives

This study generally aims for designing three wheeled chassis design, in order to achieve that following objectives are set primitively:

- Inspecting given vehicle part and its dimension
- Designing fitting components
- Drawing and Assembly of the parts on Fusion 360

- Finite Element Analysis on Fusion 360, concerning its stability
- Identifying facing problem and examine solution
- Additional computation on other parts
- Conclude the project by evaluating

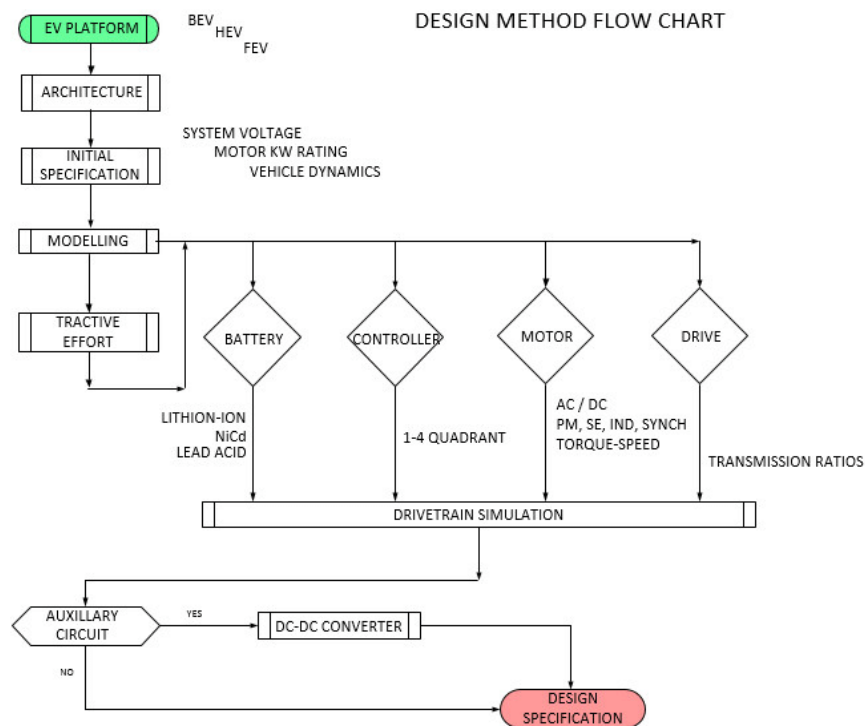
When an specific issue arises, finding a solution and iterating the process is necessary.

## 2 Methodology

CAD has become a crucial tool in engineering because it allows engineers and designers to build and alter designs fast and accurately. This enables them to visualize and test their plans quickly, make the required adjustments, and optimize them for functionality, robustness, and affordability.

Designing three-wheeled vehicles can be challenging in a way that computing stability analysis by hand instead of implementing CAD. However, it is also suitable for visualizing, assembling the parts, and general optimization.

Figure below shows flow chart which have been followed.



(4)

Figure 1: Design method flowchart

### **3 Literature review**

Many people have long dreamed about creating flying automobiles, and recent technological developments have made this dream more likely to come true. Flying cars, sometimes called vertical takeoff and landing vehicles, can completely change how people get around by allowing them to fly over great distances fast and efficiently while avoiding ground-level impediments like traffic and other roadblocks.

The development of lightweight materials, sophisticated propulsion systems, and sophisticated navigation and control systems that permit vertical takeoff and landing, steady flight, and safe operation have been the leading research focuses in this field. One recent study, for instance, discovered that carbon fiber composites significantly reduce weight compared to conventional aluminum and steel components, making them perfect for usage in flying car designs.

The development of electric propulsion systems, which provide greater efficiency and lower emissions than conventional combustion engines, has been another significant field of study. According to a recent study, the need for environmentally friendly transportation options might push the market for electric vertical takeoff and landing aircraft to \$7 billion by 2026.

Although technology has made some promising strides, many obstacles need to be cleared before flying cars can become a common form of transportation. For instance, operating these vehicles in populated regions raises regulatory severe and safety considerations; new infrastructure and flight control systems are required to ensure safe and effective operation.

The creation of flying vehicles has the potential to redefine how we see transportation by bringing new heights of comfort, effectiveness, and sustainability. To address the many remaining technological, governmental, and safety issues, extensive research and development efforts are still required.

## 4 Designing and Modelling

### 4.1 Mechanic parts

#### 4.1.1 Chassis

The chassis needs to be strong enough to sustain the vehicle's suspension system and endure cabin and battery forces. This has been accomplished using a chassis of ladder chassis kind. This chassis offers flexibility in design so that it may be changed to satisfy the required design criteria. Table 1 provides the material qualities.

Material properties	
Material type	High-strength low-alloy (HSLA) steel
Young's Modulus	205 GPa
Yield Strength	290 MPa
Density	7750 kg/m <sup>3</sup>
Ultimate Strength	434 MPa
Cross section	50x30 mm
Thickness	3mm

Table 1: Material specification

Ladder-type chassis is famous for high stiffness, ease of production, simplicity, and low body rolling effect on the vehicle when cornering. Therefore, the front chassis is designed to be as convenient as possible, as shown in the Figures below. In addition, it is designed as such so that there is sufficient space for other parts to fit in, such as the motor, battery, seats, and so on.

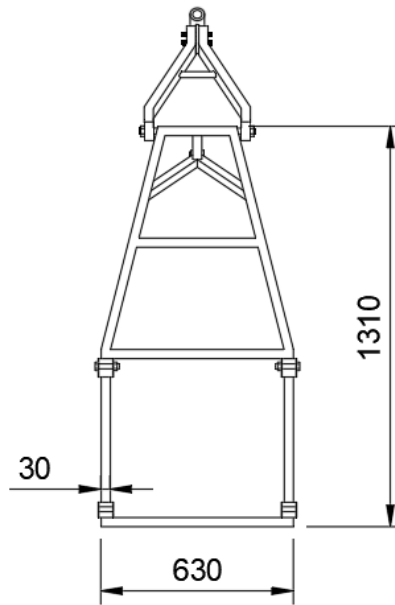


Figure 2: Top wireframe of chassis

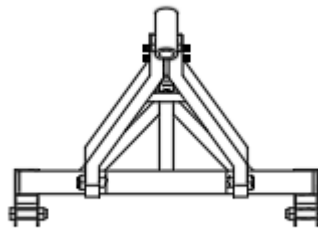


Figure 3: Rear wireframe of chassis

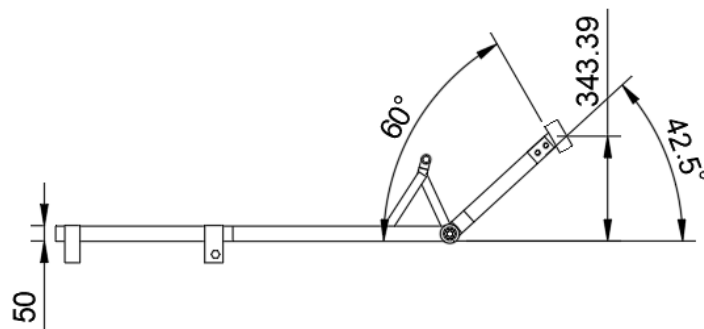


Figure 4: Side wireframe of chassis

Since vehicle is tadpole, two wheels in front and one wheel in rear, rear chassis and fork is designed as shown in figure below in order to maintain stability of swing arm type suspension.

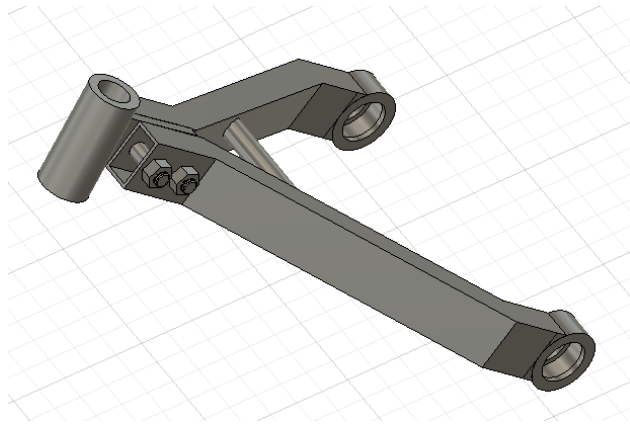


Figure 5: Rear chassis 1

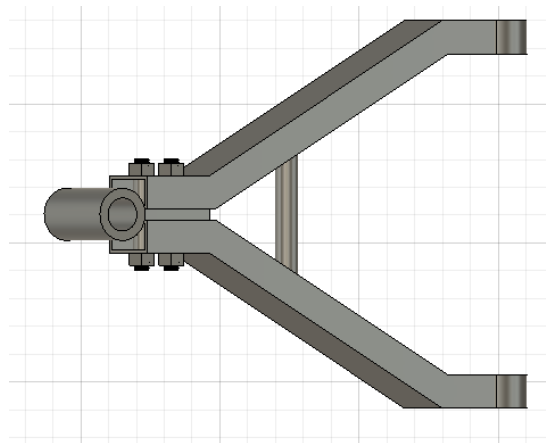


Figure 6: Rear chassis 2

#### 4.1.2 Suspension

Although there are many different kinds of suspension systems for cars, in this project the most popular kinds—simple swing arm type coil springs and leaf springs with slipper ends—are employed to support the vehicle as shown in figure below.

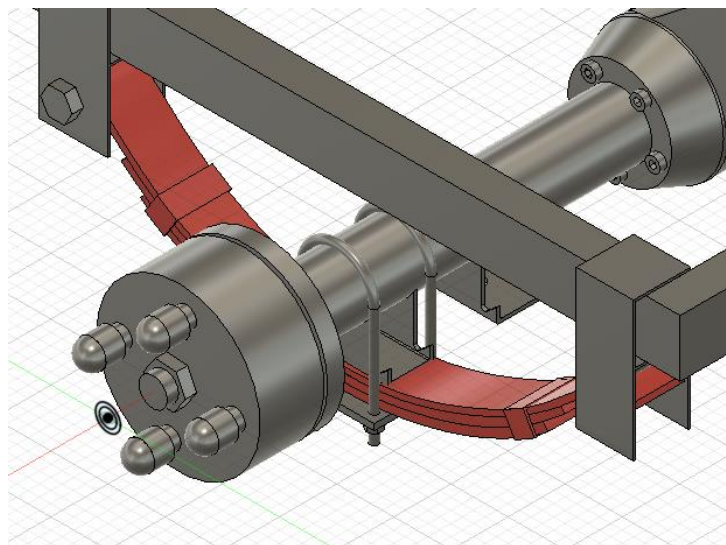


Figure 7: Leaf spring with slipper end

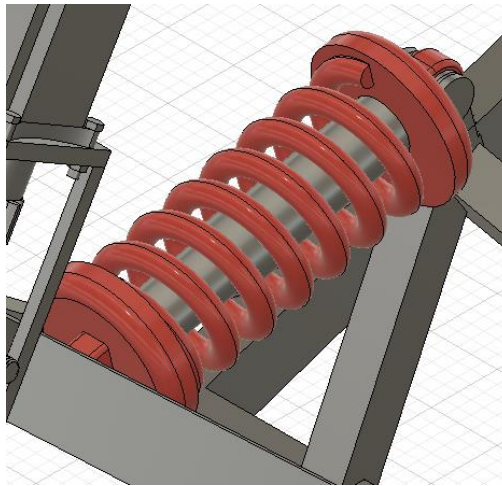


Figure 8: Coil spring

#### 4.1.2.1 Spring

A typical form of suspension system in automobiles, including cars, trucks, and motorcycles, is coil spring suspension. The method comprises a coil spring connected to the suspension arm or struts at one end and the vehicle's chassis at the other. The coil spring aims to compress and absorb road surface shocks and vibrations, giving passengers a smoother and more pleasant ride.

A vehicle's coil spring contracts when it hits a bump or uneven surface, absorbing the impact's energy and lessening the consequences on the passengers. The spring returns to its original length while the car keeps moving, helping to maintain a constant ride height and ensuring the wheels stay in touch with the ground. Because they are often dependable and straightforward to maintain, coil spring suspension systems are a popular option for various cars.

Swing arm suspension is a reliable and popular suspension system that gives passengers a smooth ride and helps shield the car's internal parts from the impact of rough roads. Depending on the particular vehicle and application, the system's design and execution may change. Still, its fundamental purpose—to dampen shocks and vibrations and maintain constant contact between the wheels and the ground—remains the same. The figure below shows the chassis frame and its FBD as how the suspension system is applied.

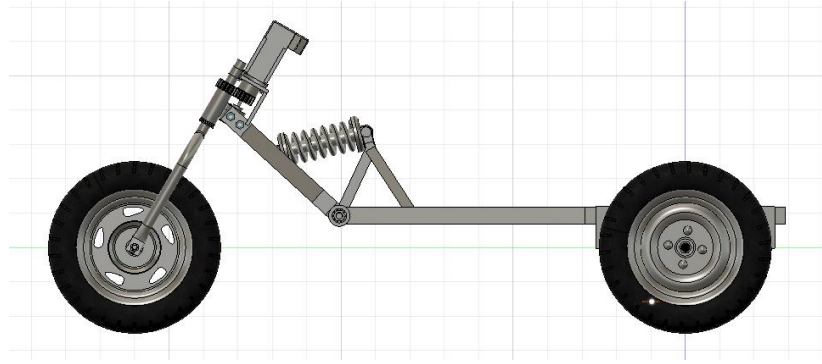


Figure 9: Right side view of vehicle

To calculate axial force on spring, FBD of front-mid chassis is used as shown in figure below.

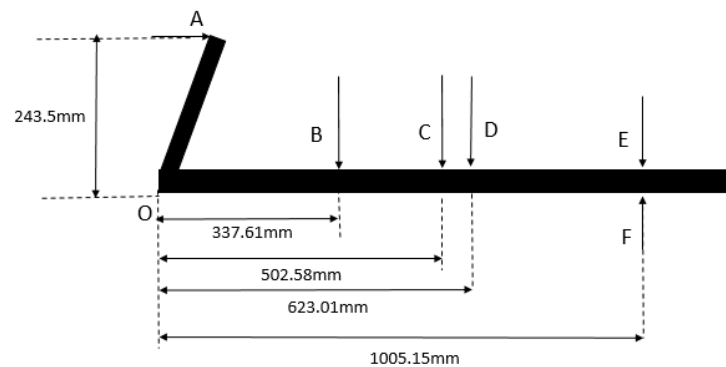


Figure 10: Free body diagram of front chassis

$F_B=1275.3\text{N}$  (Passenger and seat weight)

$F_C=588.6\text{N}$  (Vehicle frame weight)

$F_D=192.83\text{N}$  (Front chassis weight)

$F_E=824.04\text{N}$  (Battery weight)

$F_F=2492.55\text{N}$  (Front reaction force)

These values are found from simulation in section 4.3.3. As a result,  $F_A$  is found to be 3411.07N. In order to calculate spring constant and spring stress, such formulas are used: (5)

$$k = \frac{F}{y} = \frac{d^4 G}{8D^3 N}$$

$$\tau_{max} = K \frac{8FD}{\pi d^3}$$

$$K = 1 + \frac{0.5}{C}$$

$$C = \frac{D}{d}$$

,where:

d = Wire diameter

G = Shear modulus of material

D = Coil diameter

N = Number of active coil

K = Direct shear factor

C = Spring index

F = Applied axial load

From calculation, parameters are found to be:

Parameter	Value
Wire diameter, d	0.01597 m
Shear modulus of material, G	80 GPA
Coil diameter, D	0.07747 m
Number of active coil, N	7
Direct shear factor, K	1.103
Spring index, C	4.85
Applied axial load, F	3411.07 N
Spring constant, k	200000 N/m
Spring stress, $T_{max}$	182.2 N/mm <sup>2</sup>

Table 2: Coil spring specification

Since  $T_{max} < T_{allow} = 345 \text{ N/mm}^2$ , the spring design is accepted.

#### 4.1.2.2 Leaf spring

Leaf spring suspension is a system found in heavy-duty trucks, trailers, and off-road vehicles. It consists of multiple layers of curved metal strips (called leaves) attached

to the vehicle's frame at one end and to the axle at the other. The leaf springs compress and absorb shocks and vibrations from the road surface, providing a smoother and more stable ride for passengers and cargo. In addition, they are durable and can handle heavy loads, making them a popular choice for commercial and industrial vehicles. Of course, the design and implementation of the system can vary depending on the specific application. Still, the basic principle remains: to absorb shocks and vibrations and provide a smoother, more stable ride for passengers and cargo. Leaf spring load capacity is found by static simulation in section 4.3.2.

#### 4.1.2.3 Dampers

A suspension damper is essential to a car's suspension system, regulating the suspension's movement and vibrations. Its primary function is to reduce oscillations and vibrations caused by bumps, potholes, and other uneven road conditions. Vehicle suspension dampers come in various popular kinds, such as hydraulic or oil-filled dampers, gas-filled dampers, electronically controlled dampers, adjustable dampers, and air dampers. The hydraulic or oil-filled damper is the most commonly employed in automobiles, as it delivers consistent performance, is affordable, and has good damping properties for most driving situations.

Telescopic dampers are employed in this project to absorb loads and vibrations on the vehicle's rear side. A critical damping value,  $C_c$ , must be discovered to maximize vibration suppression since overdamping makes the ride seem rougher, and under damping makes the ride feel overly bouncy. Critical damping is occurred only when:

$$C_c^2 - 4mk = 0$$

which derived into

$$C_c = 2m \sqrt{\frac{k}{m}}$$

,where:

$m$  = applied mass

$k$  = stiffness constant.

Applying  $m=W/g=3411.07N /9.81 \text{ m/s}^2=347.71 \text{ kg}$  and  $k=200000 \text{ N/m}$ ,  $C_c$  is found to be  $16678.37\text{Ns/m}$ . It is impossible to ensure that it act exactly as theorotical value in

real life, but getting close to this value is the point. The dampers extended length is 270mm.

### 4.1.3 Steering system

The steering system, which is an aggregation of all the connections utilized to drive the vehicle in the appropriate direction, is discussed in this section. Vehicles with two front wheels often employ a steering arrangement to turn the front wheels using a hand-operated steering wheel placed in front of the driver through the steering column and utilizing the universal joint to deviate from the straight path. The vehicle is geometrically structured to have a fixed rolling center when turning for dynamic stability and to guide the vehicle in a specific direction.

#### 4.1.3.1 Background

To have proper steering, all perpendicular axes must be met at one point, as shown in the figures. Therefore, in our situation, it is considerably simpler to adjust steering angles for a three-wheeled vehicle. Depending on each vehicle's unique design and configuration, the steering angle comparison between 3 and 4-wheeled vehicles may differ. Due to their lower turning radius and more compact construction, 3-wheeled vehicles often have a larger maximum steering angle than 4-wheeled vehicles.

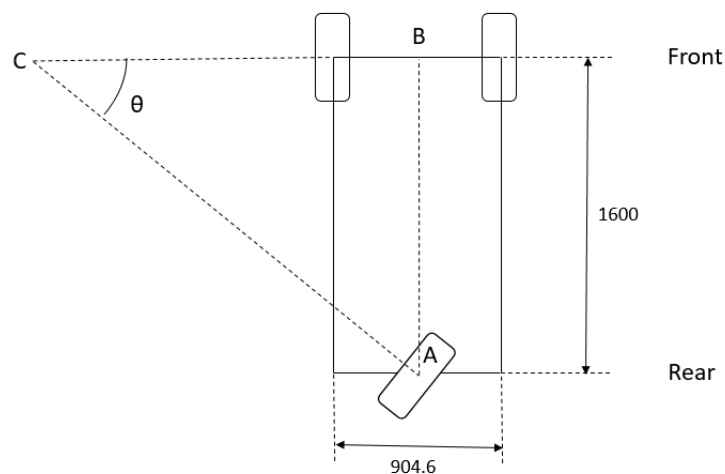


Figure 11: 3 wheeled tadpole vehicle making left turn

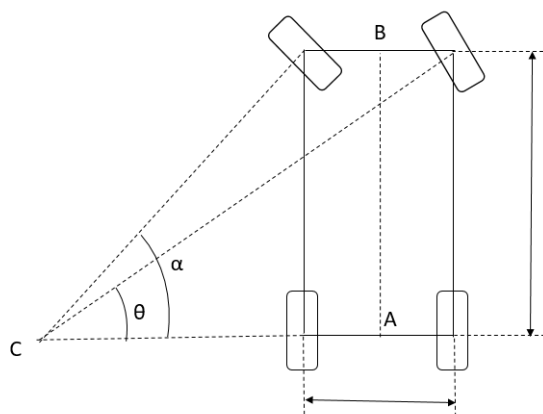


Figure 12: 4 wheeled automobile making left turn

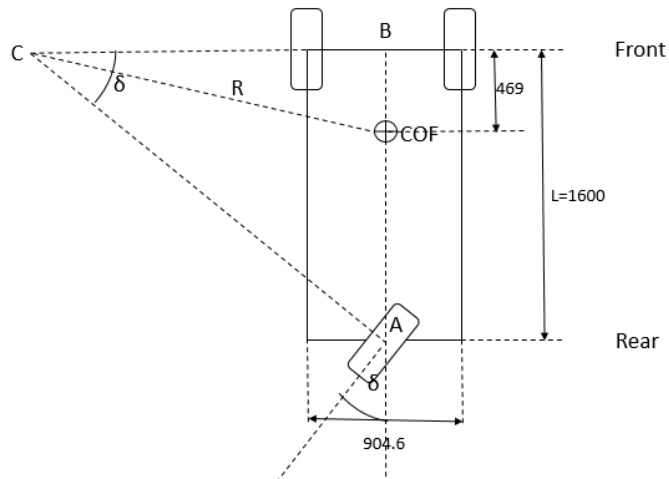
A three-wheeled vehicle's steering angle may often be up to 45 degrees or more, allowing for increased mobility in confined locations and tighter turns. This is especially helpful in urban settings or in situations where the car must maneuver through congested regions or tight roadways.

In contrast, the maximum steering angle of four-wheeled vehicles is often lower, at 30 degrees or less. This is because these vehicles need a bigger turning space due to their larger turning radii. However, for better handling and agility, some 4 wheeled vehicles, such as sports cars or other high-performance vehicles, may have a larger maximum steering angle.

#### 4.1.3.2 Understeering and Oversteering

Tadpole-shaped three-wheelers have the ability to over or understeer. The phrases oversteer and understeer are used to describe how a vehicle handles when making a turn.

When the car's front wheels lose traction, it experiences understeer, which causes it to turn less than the driver expects. Several things may bring this on, including the car's weight distribution, tire traction, or suspension geometry. If the weight distribution is skewed toward the back or the front tires do not have enough traction, understeer may happen in a tadpole design. When the vehicle's back wheel loses traction, oversteer happens, causing the car to turn more than the driver intended. Several things might contribute to this, including high speed, sudden throttle or brake inputs, or a rear weight bias. If the weight distribution is skewed toward the front or the rear tire loses traction, oversteer may happen in a tadpole layout.



It is crucial to design and calibrate the vehicle's steering and suspension systems to obtain the appropriate handling characteristics and avoid oversteer or understeer. The figure below shows the turning diagram with vehicle dimensions and steering angle, or steering angle, which are taken as  $60^\circ$  at maximum as a boundary condition. From this geometry, the relationship between the turning radius and steering angle is expressed as:

$$\tan\delta = \sqrt{\frac{L^2}{R^2 - 0.4842^2}}$$

When considering velocity, cornering, front and rear lateral forces, equation reforms:

$$\tan\delta = \sqrt{\frac{L^2}{R^2 - 0.4842^2} + K \frac{V^2}{R}}$$

Where, K is understeer gradient, V is vehicle velocity. The equation now has 3 variables:  $\delta$ , K and V. if K is negative when plugging input into other two variable, then vehicle tend to understeer, losing frontal wheel traction, on the other hand if K value is positive, vehicle will tend to oversteer, losing rear wheel traction. R is found to be 1.04666m when turning angle is maximum and neutral steering is satisfied.

#### 4.1.4 Encoder

A rotary encoder is a sensor that measures the rotational speed and angular position of a rotating shaft. It is made up of a rotating shaft and a sensor that tracks the shaft's movement and produces electrical signals that reflect it.



Rotary encoders come in two varieties: incremental and absolute. Although incremental rotary encoders don't offer a definite position, their pulses are proportionate to the shaft's rotating speed and direction. On the other hand, absolute rotary encoders provide a different digital code for each position of the shaft, enabling the determination of the absolute location of the shaft.

Applications for rotary encoders include robotics, machine tool positioning, printing presses, and automotive systems. In addition, they are frequently employed in motor control systems to provide feedback on the position and motion of the motor shaft, enabling fine motor movement control.

In our case incremental optical Hengstler RI58-O/120EK, which have 120PPR, >10mm diameter shaft, Push-Pull (HTL) or RS422 (TTL) output signal format, is selected to gauge turning wheel.

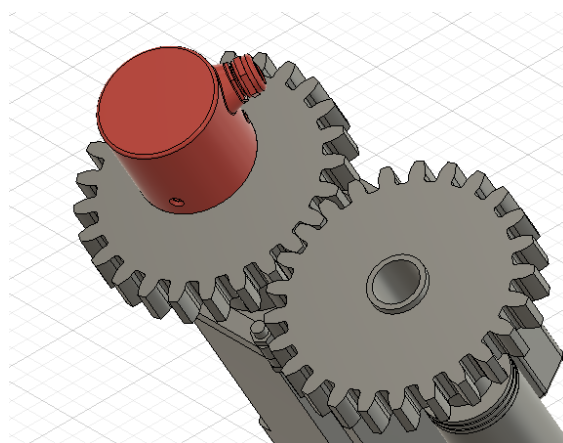


Figure 13: Encoder

#### 4.1.5 Wheel design

In this particular project, 65J 8PR tire model is used as shown in figure. Some of specifications of tire are: the tire can handle 160km/h, has 8 plies, 16x4.0inch dimensioned and fitment is 3.75-12.

Here are its main criteria for wheel design:

- Must be resilient enough to sustain centrifugal loading.
- Need to be able to handle both static and dynamic demands.
- Ensure good stability of the structure to fend off deterioration.
- To endure acceleration, braking, and turning, the grip must be excellent.



Figure 14: Front wheel



Figure 15: Rear wheel

#### 4.1.6 Brake

Many conventional vehicles and some electric vehicles use drum brakes as a standard braking system. Drum brakes are generally utilized in conjunction with the regenerative braking system, which transforms the vehicle's kinetic energy into electrical energy to be stored in the battery on the wheels of an electric car.

Drum brakes consist of a spherical drum fastened to the wheel and two curved brake shoes within. To slow down or stop the car, friction is created when hydraulic pressure is provided to the brakes, pushing the shoes outward and pressing them against the inside of the drum. Despite generally being less effective than disc brakes, drum brakes are still frequently used in electric vehicles because of their dependability, low price, and simplicity of maintenance.

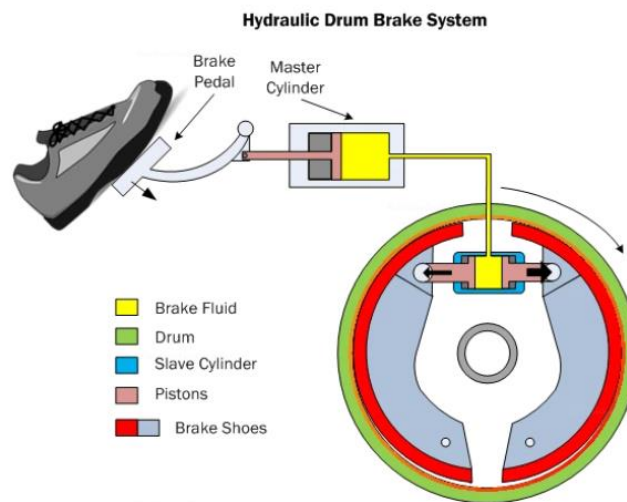


Figure 16: Drum brake mechanism

Even while they have advantages, drum brakes have certain drawbacks. They can have less effective braking since they are more prone to overheating than disc brakes. Furthermore, compared to disc brakes, drum brakes are typically less responsive and require a longer stopping distance. In order to improve performance and safety, several makers of electric vehicles have begun to switch to employing disc brakes on all four wheels.

Ratio between Braking forces acting on front and rear wheels can be expressed as:

$$\frac{F_{front}}{F_{rear}} = \frac{b + \mu h_g}{a - \mu h_g} = \frac{1.131 + 0.9 * 0.411}{0.469 + 0.9 * 0.411} = 15.18$$

,where b is distance between rear axle and vehicle COG, a is distance between front axle and vehicle COG,  $\mu$  is road abrasion coefficient,  $h_g$  is distance between ground

and COG. It is stated that when  $\mu$  is larger than 0.8, rear wheel will be locked before the front wheel locked, which tend to cause vehicle instability. (6) Thus it is preferable to push brake pedal smoothly.

In this project drum brake is used on front 2 wheels, triggered by brake wires which withstand master cylinder pressure.

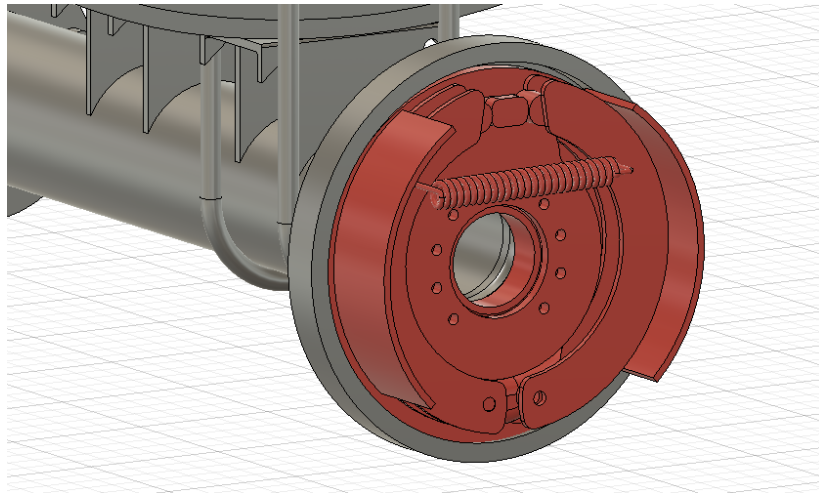


Figure 17: Front drum brake

In front, suitable brake size is 130x30mm, while 130x20mm sized brake is suitable.

#### 4.1.7 Motor

An electric motor, often known as an EV motor or an electric vehicle motor, is a device that transforms electrical energy from an EV battery into mechanical energy to move a vehicle. Brushless DC motors or AC induction motors are frequently utilized as electric motors in EVs.

Unlike gasoline engines, electric motors, which offer rapid torque, can accelerate swiftly and smoothly. In addition, they are more efficient and ecologically friendlier than gasoline engines since they emit no emissions, have fewer moving parts, and need less maintenance.

Instead of a conventional gearbox, EV motors are typically installed directly on the wheels or the transmission. They are managed by an electronic motor controller, which modifies the power sent to the motor based on input from the driver and the vehicle's speed. The range and performance of electric cars are anticipated to rise as battery technology advances, making them a more viable substitute for conventional gasoline-powered automobiles.

DC motors have the following characteristics: an identical wide range of varying speeds with the potential for simple control, the ability to reverse rotational movement, precise spin rates, and the possibility to start an adequate torque.

In order to make motor calculation, boundary conditions must set, where some of it are assumed. In table below conditions are present:

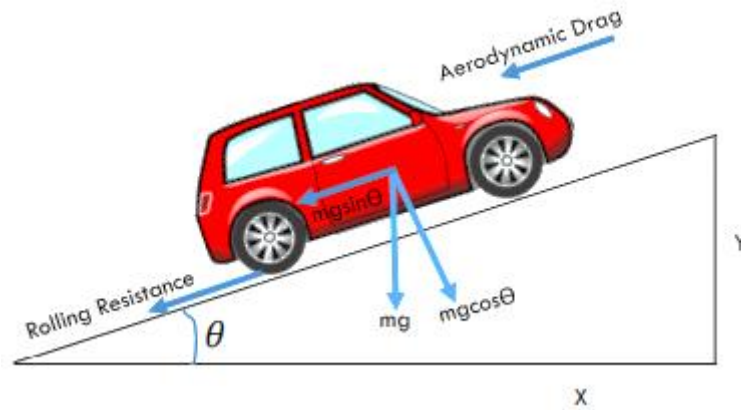
Parameters	Value
Weight	357.9kg
Max speed	60km/h
Acceleration	60km/h in 10sec
Wheel radius	0.5m
Front face area	2m <sup>2</sup>
Rolling resistance coefficient	0.02
Air resistance coefficient	0.5
Air density	1.29kg/m <sup>3</sup>
Road medium	Asphalt
Inclination angle	13°
Travel distance on single charge	80km

Calculation:

$$a = \frac{v}{t} = \frac{60\text{km/h}}{10\text{s}} = 1.667\text{m/s}^2$$

$$s = 0.5 * a * t^2 = 0.5 * 1.667\text{m/s}^2 * 10\text{s}^2 = 83.333\text{m}$$

Calculating traction forces:



Acceleration force:

$$F_a = ma = 357.9kg * 1.667 \frac{m}{s^2} = 596.5N$$

Air drag resistance:

$$F_{drag} = \frac{1}{2} * C_d * A * \sigma * v^2 = \frac{1}{2} * 0.5 * 2m^2 * 1.29 * 16.667^2 \frac{m}{s^2} = 179.17N$$

Rolling resistance:

$$F_r = C * m * g * \cos\theta = 0.02 * 357.9kg * 9.81 * \cos 0^\circ = 70.22N \text{ (68.42N in case of } 13^\circ \text{ inclination)}$$

Climbing resistance:

$$F_c = m * g * \sin\theta = 357.9kg * 9.81 * \sin 0^\circ = 0N \text{ (789.8N in case of } 13^\circ \text{ inclination)}$$

Total traction force to move a vehicle with acceleration of 1.667 m/s<sup>2</sup>:

$$F_t = F_a + F_{drag} + F_r + F_c = 845.89N \text{ (1633.89N in case of } 13^\circ \text{ inclination)} \quad (7)$$

Total traction force to move a vehicle with overcome resisting forces:

$$F = F_{drag} + F_r + F_c = 249.39N \text{ (1039.19N in case of } 13^\circ \text{ inclination)}$$

Max torque required on wheel shaft to accelerate:

$$T = F_t * r = 845.89N * 0.5m = 422.95Nm$$

Max angular speed required on wheel:

$$\omega = \frac{v}{r} = \frac{16.6 \text{ m/s}}{0.5 \text{ m}} = 33.33 \frac{rad}{s}$$

Max power required to accelerate:

$$P = \frac{F * v}{0.85} = \frac{845.89 * 16.67}{0.85} = 16586.08 \text{ Watt}$$

Power required to maintain constant velocity:

$$P = \frac{F * v}{0.85} = \frac{249.39 * 16.67}{0.85} = 4890 \text{ Watt}$$

From the calculation, final selected motor specification is shown in table below.

Parameter	Value
Model	BLDC / PMSM brushless motor HPM-10KW
Voltage	48V DC
Rated power	10-13kW
Peak power	20kW
Speed	4700 rpm
Rated torque	28 Nm
Peak torque	90 Nm
Efficiency	>85%
Cooling	Liquid cooling

Table 3: Motor specification

Peak power of selected motor higher than power required to accelerate, thus the motor is suitable.

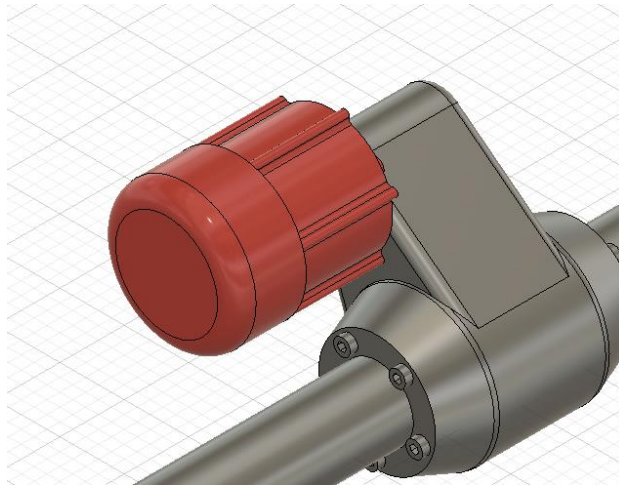
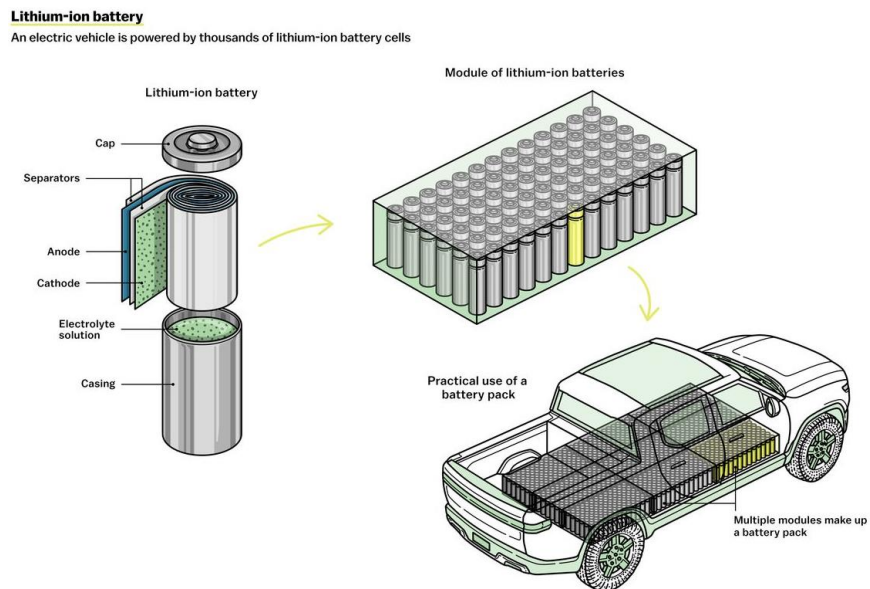


Figure 18: 48V BLDC Motor

### 4.1.8 Battery

Electric vehicles are powered by rechargeable batteries known as EV batteries or electric vehicle batteries. These batteries are made to hold electrical energy and supply it to an electric motor, which moves the car's wheels.

To provide the necessary voltage and capacity, EV batteries are often constructed from several cells linked together in series or parallel. Lithium-ion or nickel-metal hydride (NiMH) chemistry makes up the actual cells, with lithium-ion being more prevalent.



The battery capacity of an electric vehicle significantly influences its range. As a result, the content of electric cars expands as battery technology advances, making them a more competitive substitute for conventional gasoline-powered automobiles.

There are two types of lithium batteries in common. The first type employs a mixture of either nickel, manganese, cobalt, and aluminum (NMCA) or nickel, manganese, cobalt, and aluminum (NMC). Higher energy densities (energy per weight or energy per volume) are present in these batteries. Still, they also have a higher propensity to oxidize (catch fire) in the event of a severe short circuit or collision. Lithium-iron-phosphate, sometimes called LFP, is the second variety and is much more frequently utilized in China. Because iron-phosphate cells have a far lower energy density than NMC-based batteries, bigger batteries are required to produce the same amount of energy (hence driving range). The lithium-ion battery is the most popular type of battery used in EVs since it has a high energy density and a long lifespan. These batteries comprise several cells, each with an around 3.6-volt nominal voltage.

The energy density and performance of the batteries used in EVs have improved significantly over the past several decades. For instance, the Nissan Leaf, the first EV to be mass-produced, had a 24 kWh battery that allowed it to go up to 100 miles on a single charge. The Tesla Model S and Model X, two more recent EVs, can go up to 370 miles on a single charge thanks to their 100 kWh batteries. These cells are placed in series and parallel arrangements in a standard EV battery pack to produce the required voltage and capacity.

Considering an EV battery's energy efficiency is crucial since it establishes how much energy is lost when charging and discharging. A typical EV battery has an energy efficiency of 85%, which means that 15% of the energy is wasted as heat. Regenerative braking technologies and sophisticated battery management systems can also help to minimize this loss.

Mostly EV battery direct current and convert it into alternating current using inverter, but in this case, motor is already designed to be direct current thus inverter is not needed. Suitable battery for a chosen motor can be selected from previous data and further calculation.

$$\begin{aligned}
 \text{Battery Energy} &= \sum \text{Power} * \text{Time} = 16586.08W * \frac{10s}{3600s/h} + 4890W * \frac{80km}{60km/h} \\
 &= 6566.07Wh
 \end{aligned}$$

Lithium ion rechargeable cell NCM 3.7v150Ah lithium battery (8) has specification of 3.7V and 150Ah.

$$\text{Total capacity of batteries} = \frac{\text{Energy}}{\text{Voltage}} = \frac{6566.07\text{Wh}}{48\text{V}} = 136.793\text{Ah}$$

$$\text{Cell number in single series} = \frac{\text{Battery voltage}}{\text{Cell voltage}} = \frac{48\text{V}}{3.7\text{V}} = 12.97 \approx 13$$

$$\text{Number of series} = \frac{\text{Battery capacity}}{\text{Cell capacity}} = \frac{136.793\text{Ah}}{150\text{Ah}} \approx 0.912 = 1$$

Battery specification is listed below.

Parameter	Value
Battery cell	Lithium ion
Battery energy	7.215kWh
Cell nominal voltage	3.7V
Cell capacity	150Ah
Net voltage	48V
Total capacity	150Ah
Cell configuration	13(13series)
Cell cycle life	3000 times
Internal resistance	0.7mΩ
Cell dimension	149X80X88 mm

Table 4: Battery specification

Additional power need is considered sufficient enough in this battery model.

#### 4.1.9 Bearing

In rear axle, 6302 deep groove ball bearing is fit, where its static load rating is 5.4kN. In our case, rear support load is calculated to be 1.0336kN, thus the bearing is suitable.

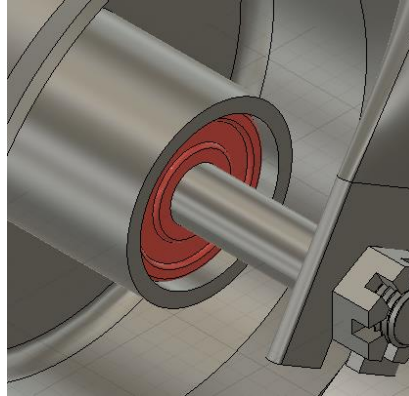


Figure 19: Rear wheel hub bearing

In front axle, 6005 deep groove ball bearing is fit, where its static load rating is 6.55 kN. In our case, front support load is calculated to be 1.246kN per wheel, thus the bearing is suitable.

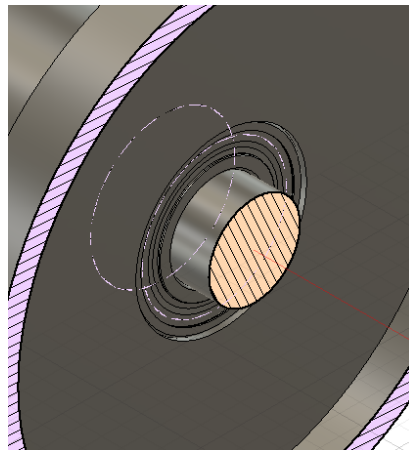


Figure 20: Front wheel hub bearing

At chassis bending area, NJ 2304 ECP cylindrical roller bearing is selected where its static load rating is 38kN. In our case, front support load is calculated to be 1.9875kN per wheel, thus the bearing is suitable.

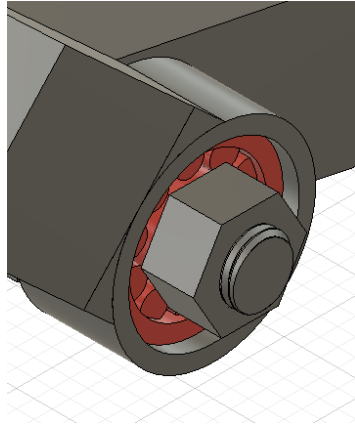


Figure 21: Chassis bearing

#### 4.1.10 Other components

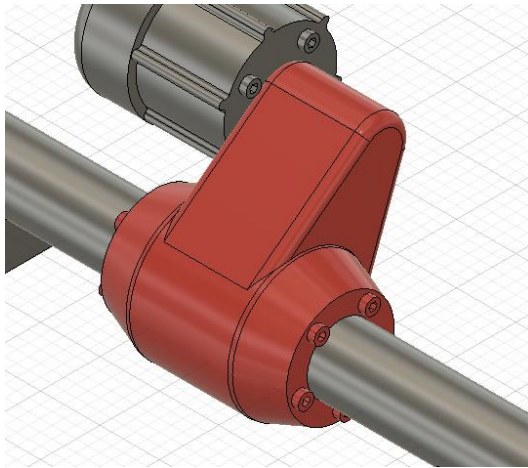


Figure 22: Differential

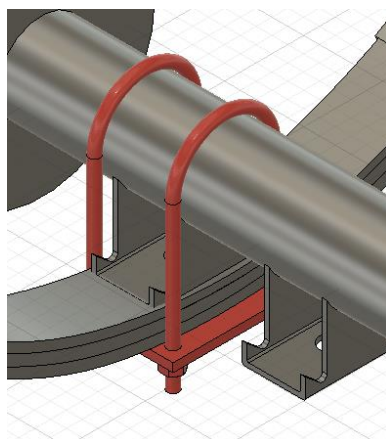


Figure 23: Central U shaped clamp

At fork area, 51106 thrust ball bearing is mounted where its static load rating is 43kN. In our case, support load is calculated to be 3.975kN per wheel, thus the bearing is suitable.

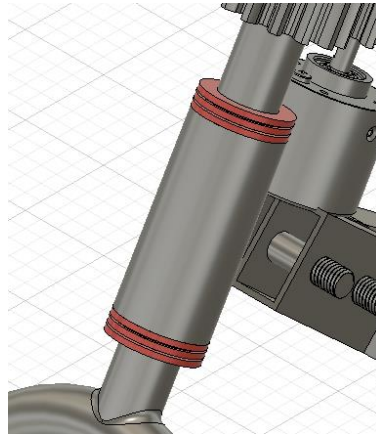


Figure 24: Thrust bearing

Spur gears mounted on fork and steering motor have these specifications:

Pressure angle	14.5°
Module	5
Number of teeth	25
Gear thickness	20mm
Pitch diameter	125mm

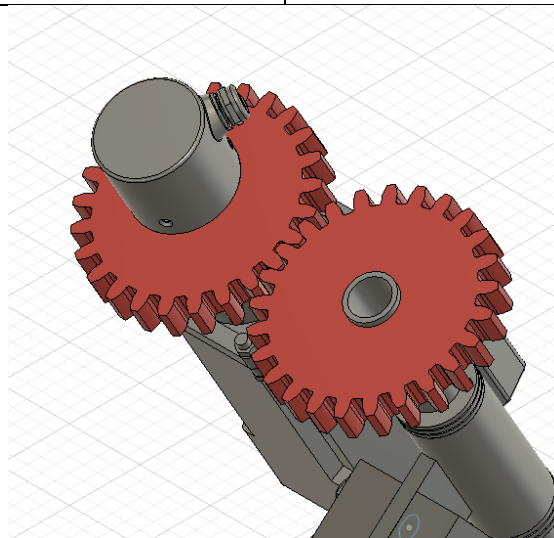


Figure 25: Spur gear

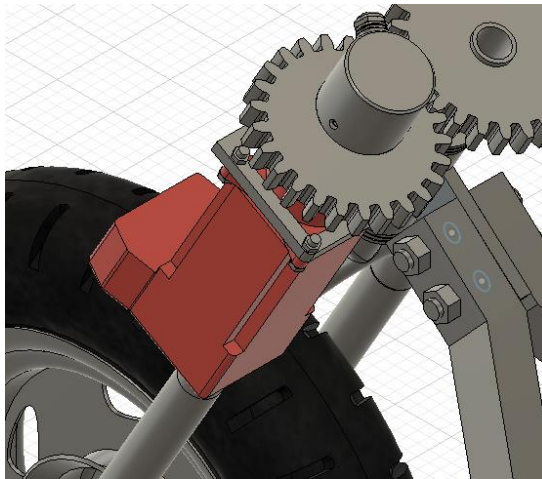


Figure 26: Electric power steering (Model EPS090)

## 5 Procedure

### 5.1 Modelling

The foundation of 3D modeling is that virtual representations of real-world locations or things may be made using digital technologies. Therefore, an accurate, comprehensive, and realistic digital model should be produced as the result of 3D modeling so that it may be utilized for various tasks, including product design, engineering analysis, and virtual prototyping.

Compared to conventional design approaches, CAD software enables designers to build, alter, and analyze digital models with improved accuracy and efficiency. Furthermore, using real-time model sharing with other designers and engineers, CAD software also enables designers to collaborate. The Figure below shows the primary sequence and structure of 3D designing.

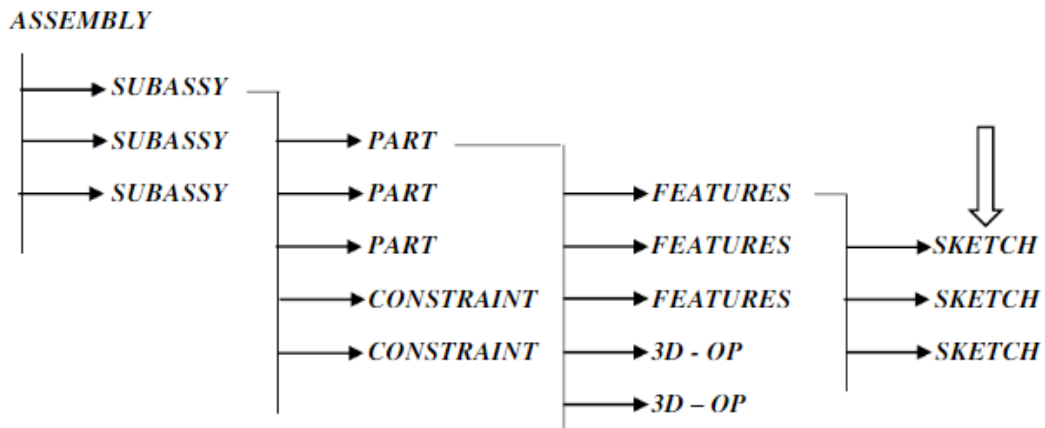


Figure 27: CAD designing structure

The usage of parametric modeling is a critical component of 3D modeling. Designers may develop models using parametric modeling based on factors or rules like the size, shape, and material characteristics of a part. Because modifications to one component of the model may instantly update other portions of the model, this enhances design flexibility and efficiency.

In general, 3D modeling is founded on the notion that digital technology may produce precise, thorough, and realistic representations of actual things and situations. As a result, the design process may be more effective, flexible, and collaborative, which can aid in developing better systems and products by designers and engineers.

## 5.2 Weight distribution

During the process of simulation, vehicle parts weight and its distribution is important in order to get correct result. In this vehicle, parts can be divided into 2 types: sprung mass, which suspended by spring and damper, and unsprung mass which is only suspended by tire elasticity. Table below shows list of the items which are sprung and unsprung mass.

<b>Sprung mass</b>	
Parts	Weight in g
Front chassis	19670.44
Rear chassis	6096.33
Batteries	50000
Car body	60000
Seats	30000
Passenger	100000
<b>Unsprung mass</b>	
L rim	2885.48
L tire	4432.27
Rear drum	8512.82
Rear shaft	6742.12
R rim	2885.48
R tire	4432.27
Motor	12083
Differential	8840.36
Front Rim	2885.48
Front tire	4432.27
Spur gear1	284.5
Spur gear2	449.43
Thrust bearing	133.28
Fork	6874

EPS	10017.74
Encasing	554.23
Drum brake1	1187.03
Drum brake2	1187.03
Damper	1171.16
Central clamp1	417.66
Central clamp1	417.66
<b>Suspension</b>	
Suspension	3521.75
Leaf spring1	3220.2
Leaf spring2	3220.2
<b>Total</b>	
	<b>356554.19</b>

Table 5: List of component mass

It is stated that, “In order to ensure the lateral stability of a three wheeled vehicle with two wheels in the front, the mass center must be located somewhere in the front third of the vehicle“ (9), where we can satisfy this condition as shown in Figure below.

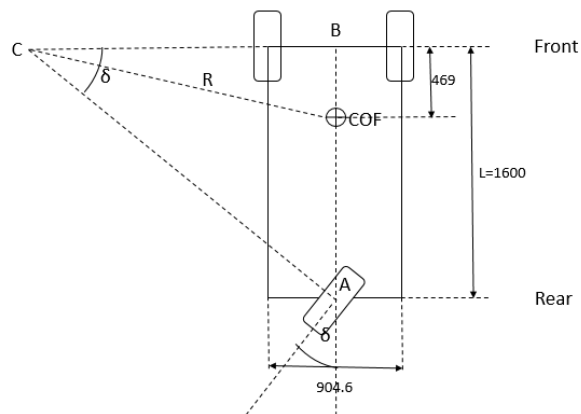


Figure 28: Center of mass of vehicle

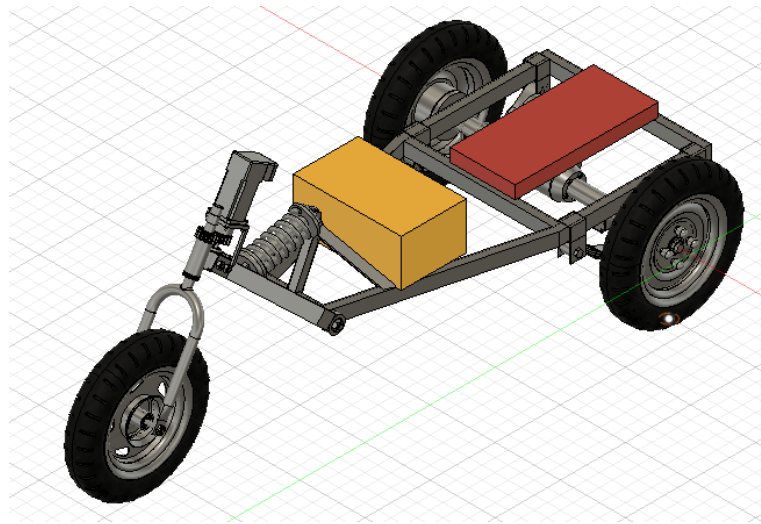


Figure 29: Weight distribution

In Figure 5, yellow block represents passenger and seat weight, while red block represents vehicle battery.

In Figure 6, reaction forces and vehicle weight is shown, from here reaction forces are found to be:  $R_1=2492.55N$ ,  $R_2=1033.6N$ , meaning that front wheels contributes 70.68% of vehicle weight (each wheel with 1246.28N) and rear wheel contributes 29.32%.

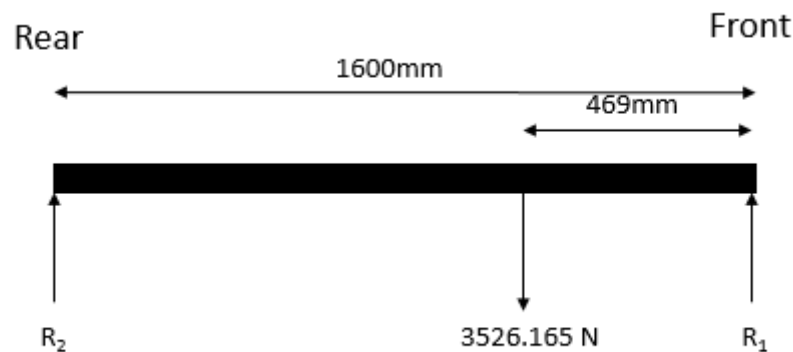
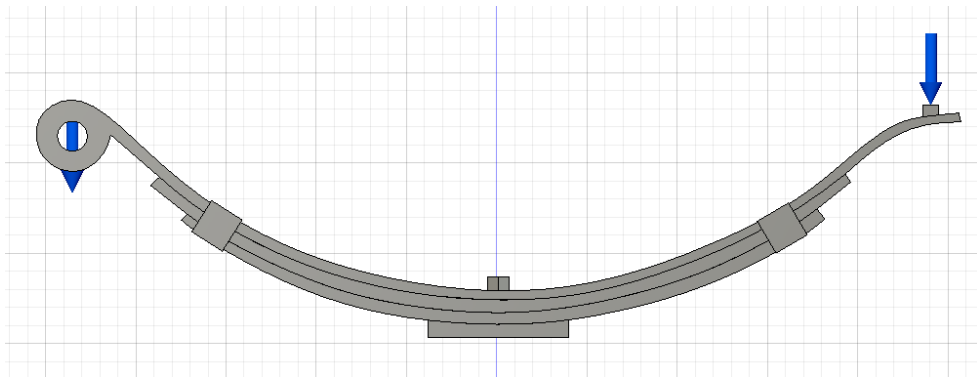


Figure 30: Vehicle side view FBD

## 5.3 Static simulation

### 5.3.1 Leaf spring

Slipper spring is implemented on front shaft of the vehicle in order to absorb road surface shocks and vibrations to give passengers and package a smooth, stable drive. In figure below, how loads and reaction forces are applied to simulate the spring is shown. Load are given 594.7N at each point since there are 2 leaf springs supporting the system. Consequently, reaction force is 1246.28N.



As a result, maximum stress on leaf spring is 108.9MPa with minimum safety factor 2.533 on small area which is acceptable since its yield strength is 290Mpa as it is shown in figure. Other areas have relatively high safety factor ensures that the spring is relatively safe.

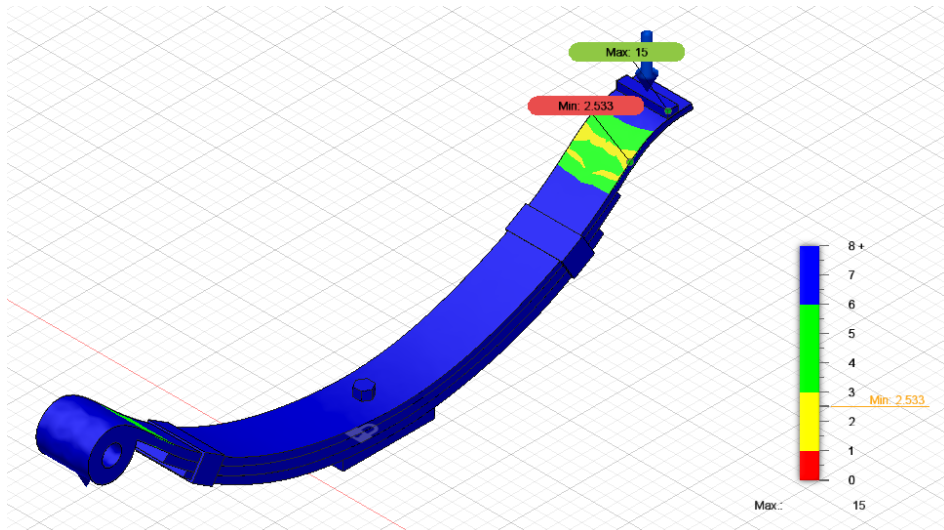


Figure 31: Leaf spring safety factor

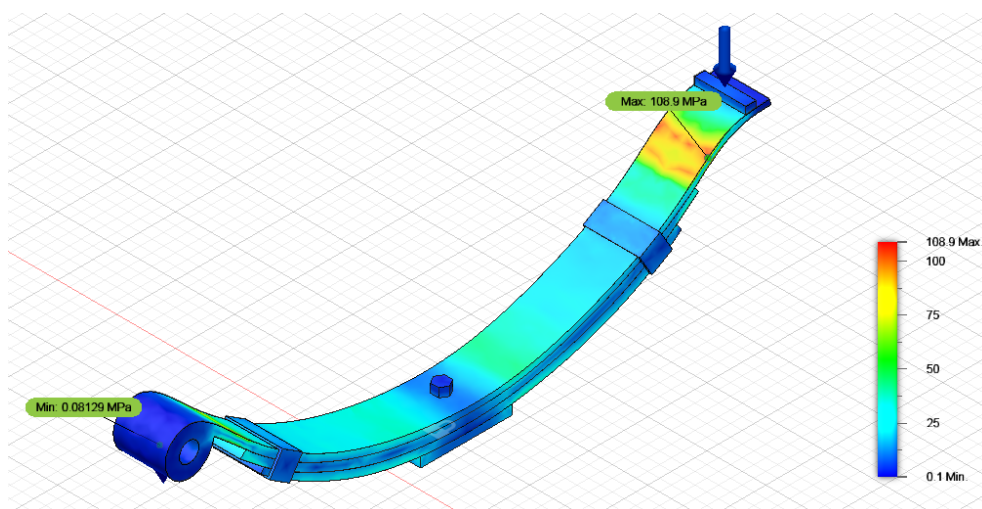


Figure 32: Leaf spring stress

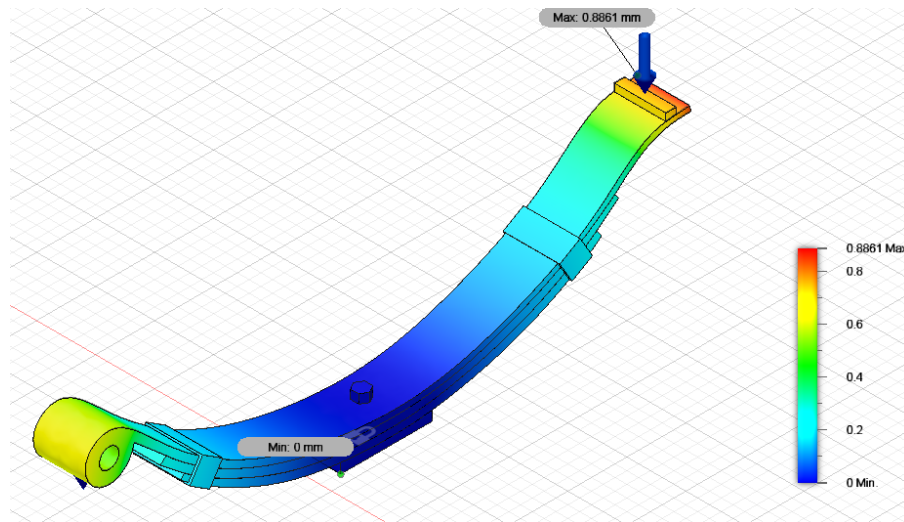


Figure 33: Leaf spring displacement

## 5.3.2 Chassis analysis

### 5.3.2.1 Bending simulation

In order to perform bending simulation, most CAD software adheres to the guidelines of FEA. FEA entails disassembling a complicated system into smaller, simpler components and using mathematical equations to forecast the system's behavior under various circumstances. It is frequently used in the engineering and industrial sectors to optimize designs, cut costs, and enhance the performance and safety of products. This technique requires boundary conditions such as constraints and mesh size. Fusion 360 is fully capable of doing simulations, including static simulation, dynamic event simulation, thermal simulations, and so on.

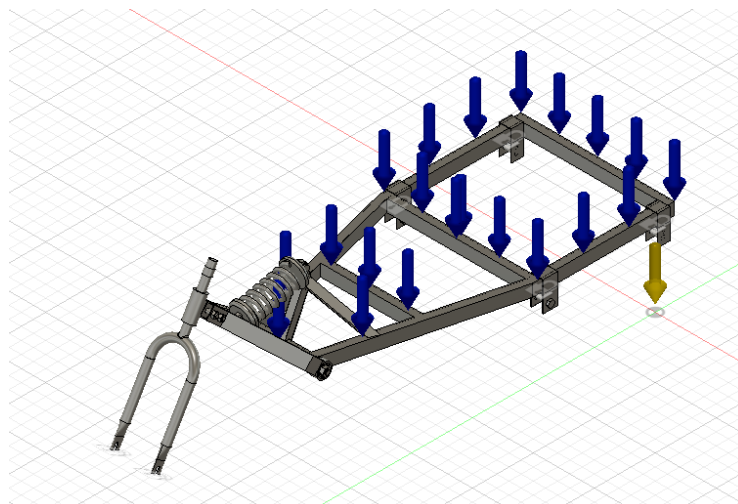


Figure 34: Bending test boundary condition

The figure above shows boundary conditions: load forces and fixed points where the front and rear wheel is supported. The safety factor is recommended to be above three at every mesh; as shown in the figure below, this condition is fulfilled. In this case,

the material's yield strength is considered a safety factor reference. Thus, it is shown that it is sufficiently safe in terms of stress even a bit more weight is applied to the chassis. The force exerted under actual circumstances has been recreated as boundary conditions. Net deformation results from total force acting on the chassis where the maximum displacement is 0.4549mm. For this type of chassis design, where the upper body is fixed to the chassis at a later stage, this value can be regarded as optimal; bending can then be reduced.

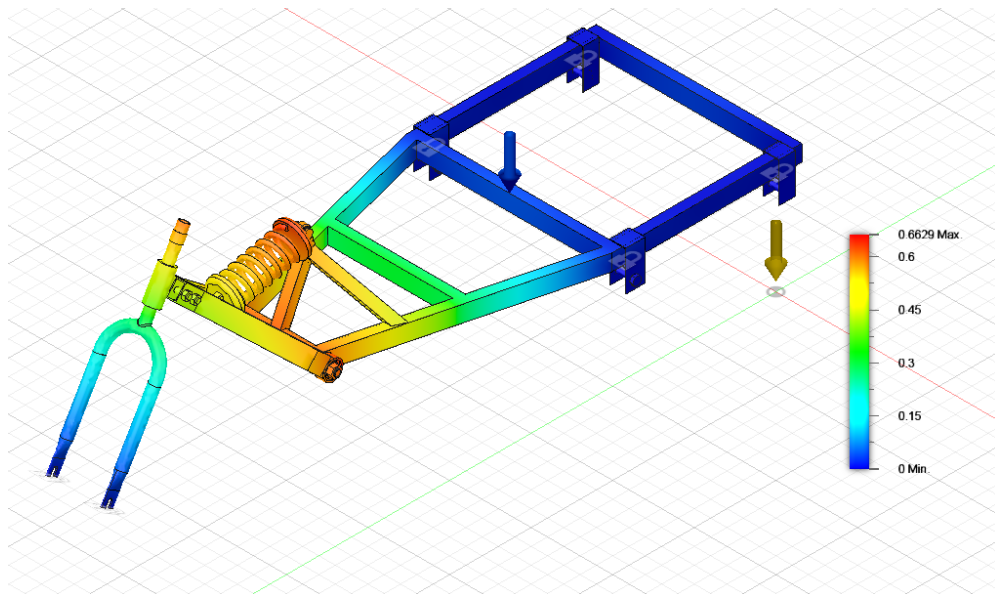


Figure 35: Chassis displacement bending test

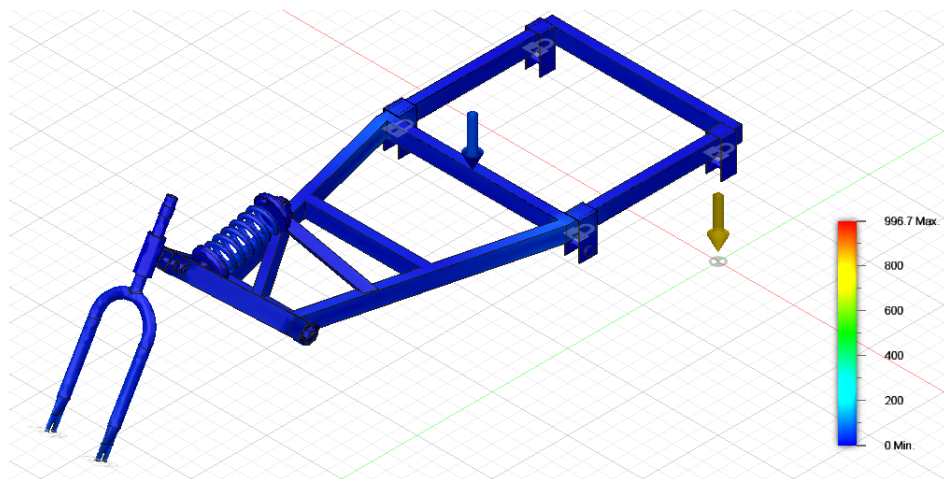


Figure 36: Chassis stress bending test

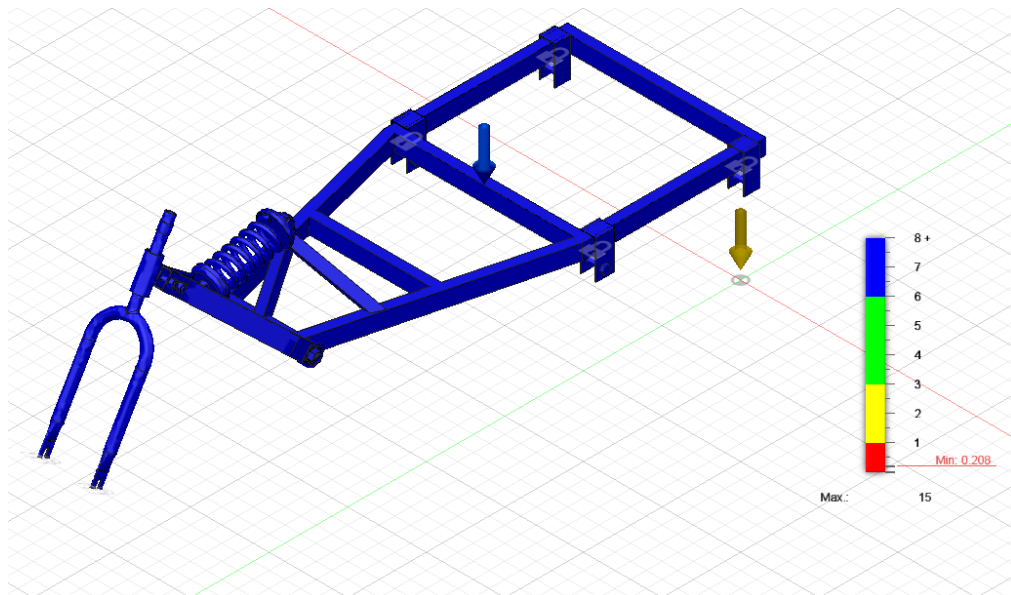


Figure 37: Chassis safety factor bending test

### 5.3.2.2 Torsion simulation

Torsional stiffness is essential for chassis design and significantly impacts vehicle ride, comfort, and performance. Hence, it is standard to conduct torsion testing to measure this factor. However, due to the complexity of intersecting cross-sections in a chassis, it can be challenging to analyze torsional rigidity analytically.

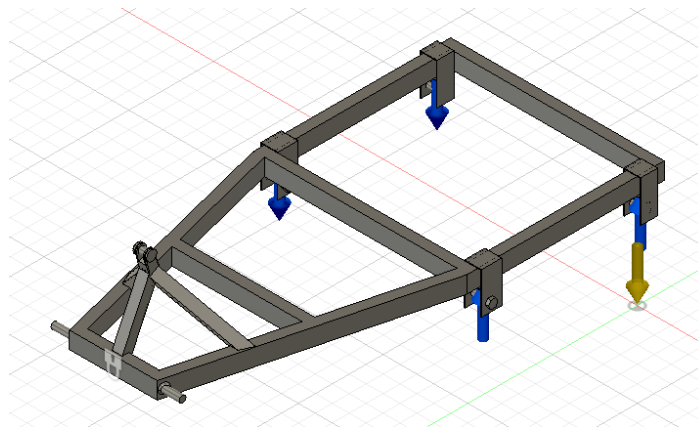
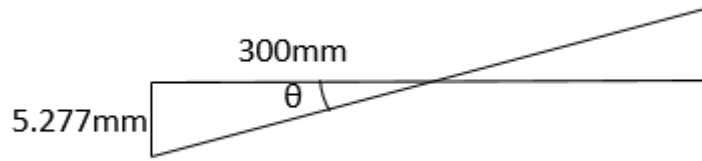


Figure 38: Torsion test boundary condition

Since maximum displacement is 5.277mm from simulation, angle of twist is calculated to be:

$$\theta = \arctan \frac{5.277\text{mm}}{150\text{mm}} = 2.015^\circ = 0.035\text{rad}$$



2.015° can be regarded as acceptable for this type of chassis design, where the upper body is fixed to the chassis at a later stage, bending can then be reduced. The system is acceptable since the maximum stress measured is 94.46MPa, which is smaller than the maximum stress permitted by steel which is 290MPa.

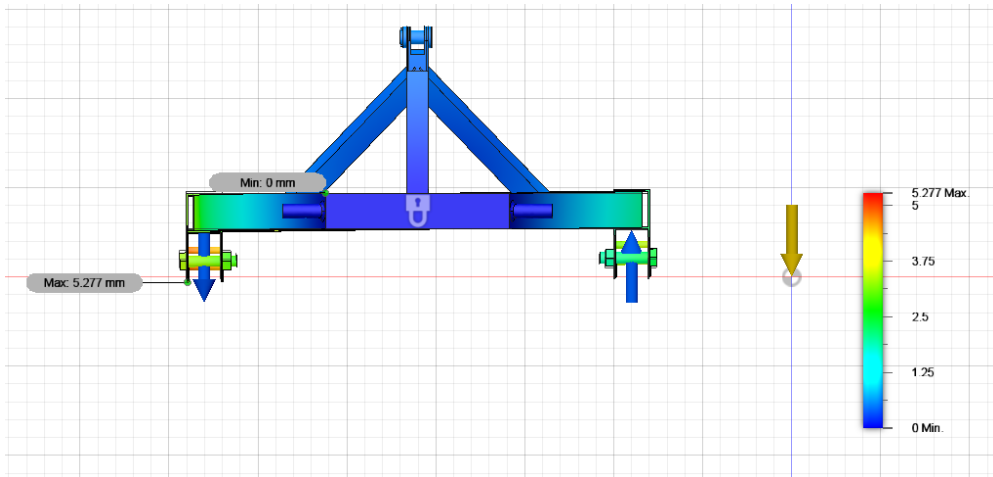


Figure 39: Chassis displacement torsion test Rear view

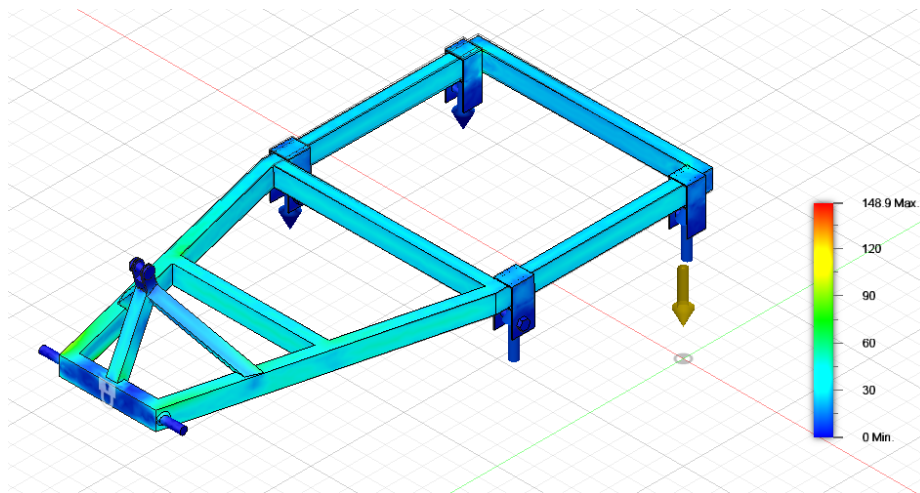


Figure 40: Chassis stress torsion test

## 5.4 Dynamic simulation

### 5.4.1 Terrain ability

In order to evaluate the car's capability to traverse rough terrain using only the back wheel drive, a comprehensive terrain assessment was carried out. The assessment aimed to assess the car's performance across diverse road conditions, encompassing road bumps, potholes, and slopes.

The results of the assessment can be observed in the series of Figures presented below, showcasing the car's maneuverability and stability in challenging terrain scenarios. These findings provide valuable insights into the car's suitability for navigating rough terrains and its potential for off-road capabilities.

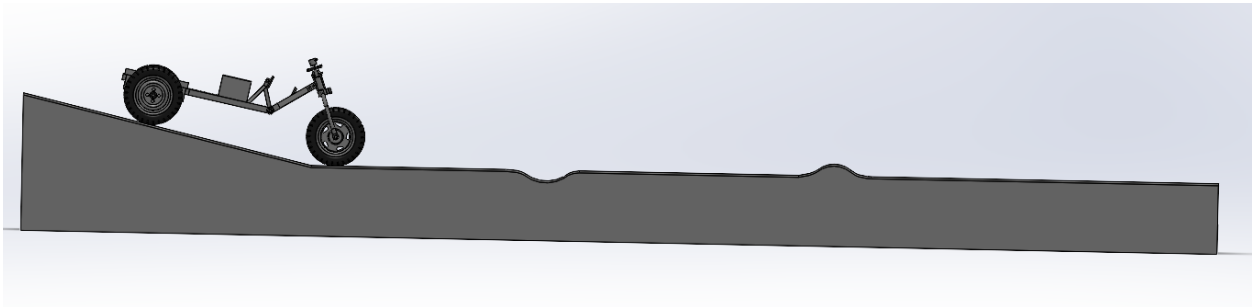


Figure 41: Terrain ability (a)

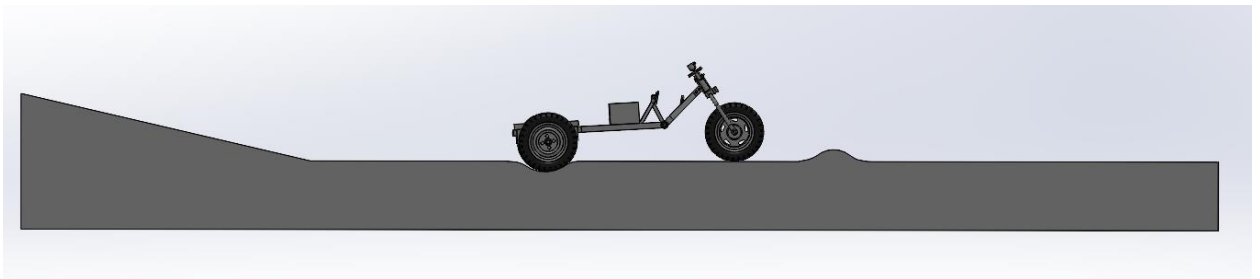


Figure 42: Terrain ability (b)

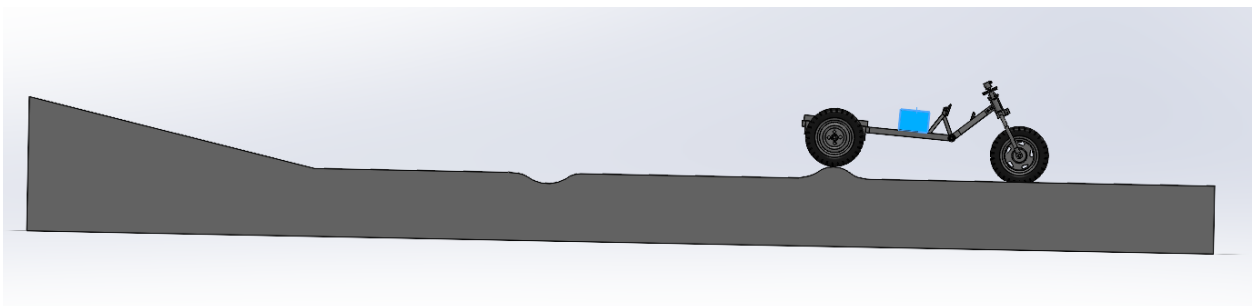


Figure 43: Terrain ability (c)

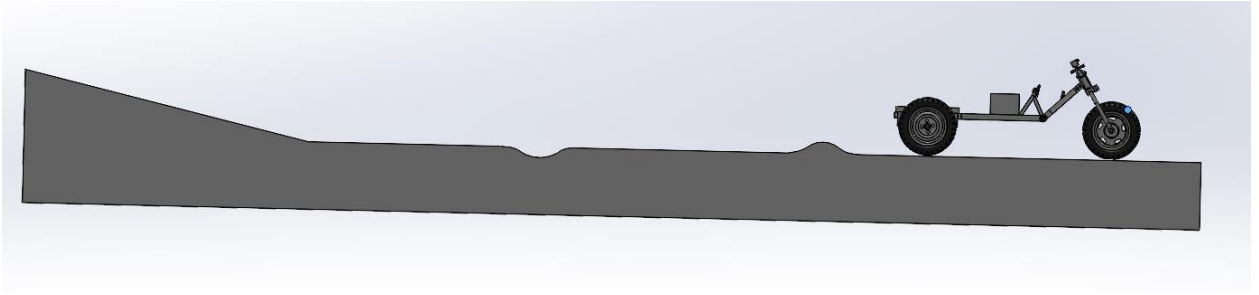


Figure 44: Terrain ability (d)

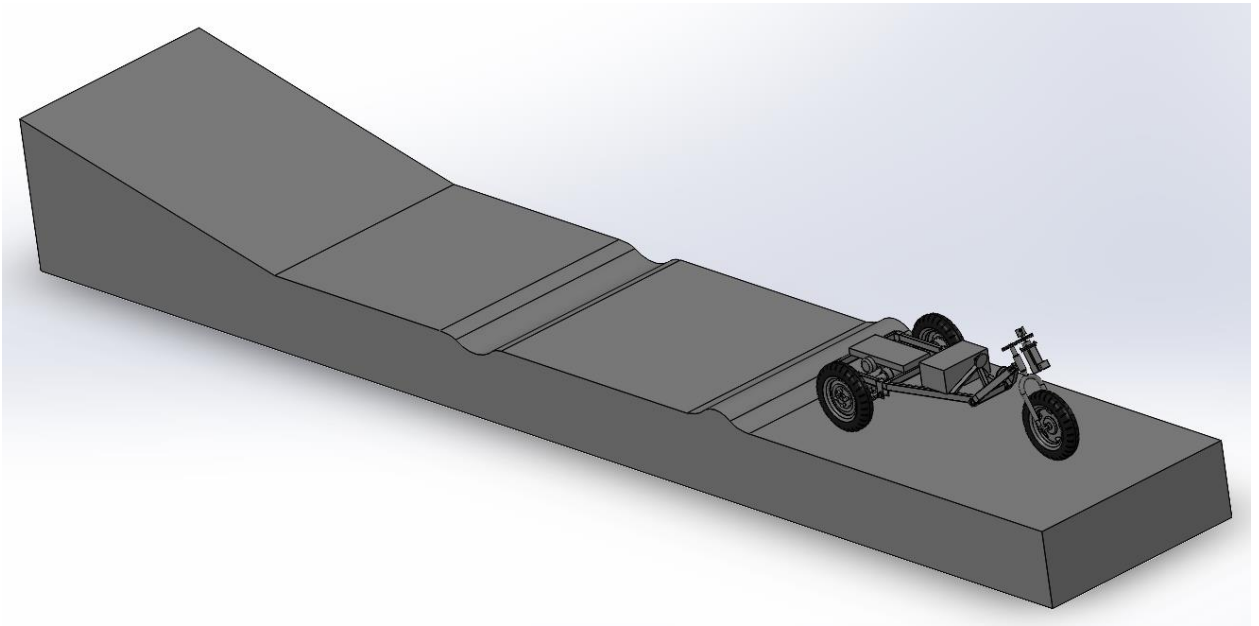


Figure 45: Terrain ability (e)

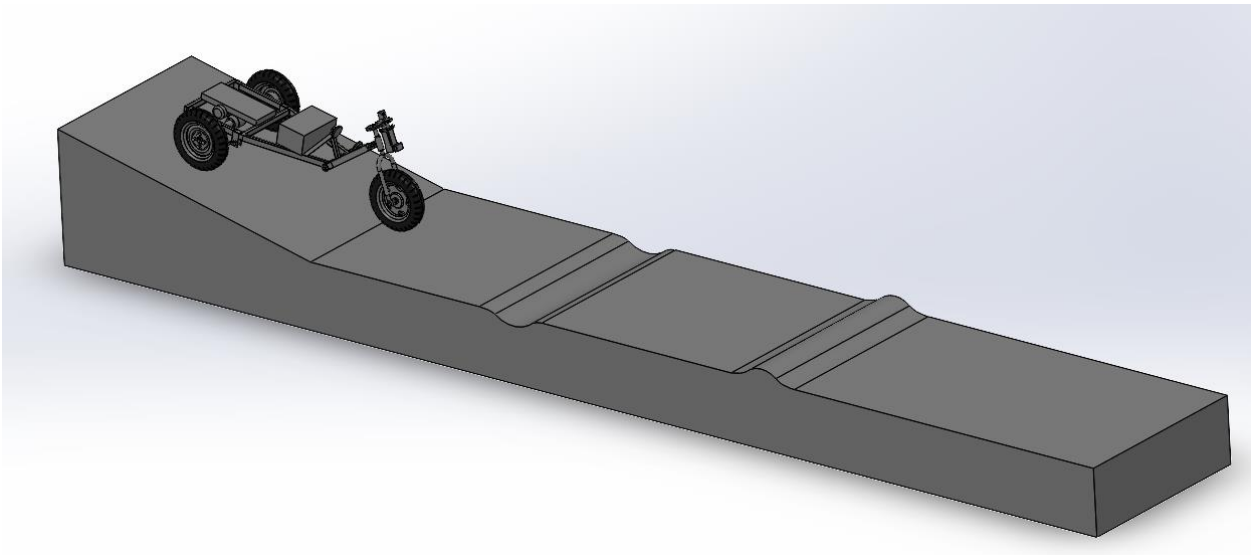


Figure 46: Terrain ability (f)

## 6 Results and Discussion

After evaluating the analysis of various types of chassis frames available, the idea of selecting the ladder-type chassis frame was narrowed down. The advantages of the ladder-type chassis frame were kept in mind, and discussions will be done on those advantages to justify the selection. Since the primary aim of the vehicle is to provide a convenient production, the ladder frame is the simplest and cheapest available on the market without compromising the strength. The torsional stiffness of the chassis frame is low, which is desirable; however, torsional rigidity is lower, making it difficult to deal with bumps, the main purpose of this vehicle is simple commuting. Therefore, certain compromises are considered.

HSLA steel has been chosen as the material for the time being with the intention of testing it against alternative materials. Because steel is stronger and more rigid than other materials, which are needed for the ladder-type of chassis, steel was chosen for the primary test. Additionally, it is the most affordable material utilized in the construction of car chassis.

Fusion 360 was used for the design and adjustments. This section will discuss the benefits of redesigning several car components.

- Frontal part of chassis is positioned comparatively low so that, leaf springs are located below the front shaft.
- Chassis are separated into front and rear type ensuring that swing arm coil spring suspension is used for rear suspension.
- Initially 2 coil spring were designed for rear suspension, but due to spacing of the vehicle this design is eliminated.
- Shock absorbers were given a tilt to boost the rigidity of the shock absorbers and springs.
- 

### 6.1 Further study

Numerous further study can be performed in order to improve accuracy of this project and to develop moreover:

- Chassis can be examined with other type of material such as aluminum for comparison of strength and weight of the vehicle.
- Chassis beam shape can be modified in order to increase strength.

- Vehicle frame can be modeled for decreased drag resistance.
- Vehicle crash test can be performed in other type of simulation software.
- Suspension system can be improved by alternative design.
- A vehicle may be utilized for various purposes.

## 7 Conclusion

In this paper, the chassis design of three-wheeled electric devices is performed. This task is executed using a methodology mentioned in Chapter 2 and several CAD software, including Fusion 360 and SolidWorks. Furthermore, EV chassis, other components regarding performance, and static/dynamic simulation are designed and carried out in this project. Here is a summary of the highlights mentioned below:

- 50x30mm steel beam ladder-type chassis is used for the optimum safety factor, low body rolling effect, and economics.
- The complete chassis design is performed from scratch using Fusion 360 software.
- Leaf slipper spring and coil spring type suspension are used in front and rear axles, respectively.
- Considering vehicle specification, 48V BLDC motor and lithium-ion electric battery calculation is performed.
- Design is implemented in view of different standards and considerations.
- Parts are designed using an analytic and mathematical approach.
- Static and dynamic simulations are performed using Fusion 360 and SolidWorks, ensuring safety.
- Terrain ability simulation is executed on SolidWorks.

## 8 References

1. Electric Vehicle Market Size, Share & Trends Analysis Report. , International Energy Agency; 2020.
2. BULUCEA CA. Energy and Exergy Efficiencies. WSEAS TRANSACTIONS on ENVIRONMENT and DEVELOPMENT. 2008 March;; 247-258.
3. WILLIAMS J. THE EARTHBOUND REPORT. [Online].; 2019 [cited 2023 May 14. Available from: <https://earthbound.report/2019/03/12/the-role-of-three-wheelers-in-sustainable-urban-transport/>.
4. Burrige M AS. The Design and Construction of a Battery Electric Vehicle. IOP Conference Series: Earth and Environmental Science. 2017 Jul; 73(012016.).
5. Norton RL. Machine Design Integrated Approach: Pearson; 2010.
6. Gao Y, Chu L, Ehsani M. Design and Control Principles of Hybrid Braking System for EV, HEV and FCV. 2007 IEEE Vehicle Power and Propulsion Conference. 2007 Sep;; 384–91.
7. Jayesh S. Renge RPRSVBSPB. Design and Fabrication of Foldable Electric. IJARIIE- ISSN(O)-2395-4396. 2017; III(3): 2699-2733.
8. Alibaba. [Online].; 2023 [cited 2023 4 30. Available from: [https://www.alibaba.com/product-detail/NMC-3-7v-CATL-100ah-116ah\\_1600468441004.html?spm=a2700.7735675.0.0.37b5CTelCTel7d&s=p](https://www.alibaba.com/product-detail/NMC-3-7v-CATL-100ah-116ah_1600468441004.html?spm=a2700.7735675.0.0.37b5CTelCTel7d&s=p).
9. Jeffrey C. Huston BJGaDBJ. Three Wheeled Vehicle Dynam. SAE Transactions. 2021 Sep; 91(820139): 591-604.